



## Supplementary Materials for

### **Reducing the metabolic rate of walking and running with a versatile, portable exosuit**

Jinsoo Kim\*, Giuk Lee\*, Roman Heimgartner†, Dheepak Arumukhom Revi†, Nikos Karavas, Danielle Nathanson, Ignacio Galiana, Asa Eckert-Erdheim, Patrick Murphy, David Perry, Nicolas Menard, Dabin Kim Choe, Philippe Malcolm‡, Conor J. Walsh‡

\*These authors contributed equally to this work.

†These authors contributed equally to this work.

‡Corresponding author. Email: pmalcolm@unomaha.edu (P.M.); walsh@seas.harvard.edu (C.J.W.)

Published 16 August 2019, *Science* **365**, 668 (2019)

DOI: 10.1126/science.aav7536

#### **This PDF file includes:**

Materials and Methods  
Supplementary Text  
Figs. S1 to S5  
Tables S1 to S7  
Captions for Movies S1 to S3  
Captions for Data S1 to S6  
References

#### **Other Supplementary Material for this manuscript includes the following:**

(available at [sciencemag.org/content/365/6454/668/suppl/DC1](http://sciencemag.org/content/365/6454/668/suppl/DC1))

Movies S1 to S3 (.mp4)  
Data S1 to S6 (.pdf, .zip, and .xlsx)

## Materials and Methods

### Functional apparel components of the exosuit

The functional apparel components of the exosuit consist of a spandex base layer, a waist belt, two thigh wraps, a battery pouch and a load-carrying belt with shoulder straps (fig. S2, movie S3, data S1). The base layer incorporates high-friction panels (NuStim, FabriFoam, PA, USA) to help the exosuit remain attached to the pelvis. The waist belt and thigh wraps are constructed with layers of an inextensible, abrasion-resistant plain-weave textile and a lightweight sailcloth material. The thigh wraps can be adjusted with laces and a tensioning dial (L4, Boa Technology, Inc., CO, USA). The waist belt can be tightened using a Velcro fastener. The load-carrying belt (Tactical Belt, VC-Time, USA) carries the actuation unit on the back. The battery is mounted on the wearer's abdomen. By having the actuator on the back and the battery pack on the front of the wearer, the entire mass of the system can be kept close to the center of mass (CoM) of the wearer. Participants wear their own running shoes.

### Actuation system and sensors

Hip extension assistance is applied by a two-degree-of-freedom actuation system. Each degree of freedom consists of an electronically commutated 4-pole power motor (#305013, Maxon, Switzerland, data S2 and S6) connected to a gearbox with a 51:1 ratio (#326664, Maxon, Switzerland) driving a 40-mm-radius multi-wrap pulley. An incremental encoder (#225778, Maxon, Switzerland) that operates at 2000 counts per revolution measures motor position. A servomotor driver (Gold Twitter, Elmo Motion Control, Ltd., Israel) controls each motor in a closed loop. A replaceable battery consisting of two 6-cell lithium polymer units (3.7 A·h) is carried in a pouch on the abdomen, which lasts approximately 7.5 km when the exosuit is actuated with a peak force of 300 N per step. Bowden cables transmit forces from the actuation unit to attachment points on the waist belt and the thigh wraps. Two load cells (LSB200, FUTEK Advanced Sensor Technology, Inc., CA, USA) measure tensile forces that are applied between the exosuit components. Two inertial measurement units (IMUs) (MTi-3 AHRS, Xsens Technologies B.V., Enschede, the Netherlands) on the anterior part of the thigh are used for gait event detection. A third IMU on the abdomen is used for estimating the motion of the CoM to distinguish between walking and running.

### Control system

The controller is designed to deliver a consistent hip extension force profile during the gait cycle. An IMU-based algorithm detects the timing of maximum hip flexion based on changes in the sign of angular velocity from the thigh IMU (26). A force-based position controller applies a hip extension force profile with desired onset, peak, and end timings by adjusting the timing and magnitude of the motor position profile on a step-by-step basis (26). The desired peak force was fixed at 300 N. This peak force was chosen based on the actuator and transmission specifications, as well as comfort considerations of the human-exosuit interface. The profiles do adapt to changes in the duration of each stride, but the profile shapes do not vary based on changes in walking or running speed. During walking, this force-based position control resulted in  $0.125 \pm 0.039$  W kg<sup>-1</sup> average positive power per side,  $-0.003 \pm 0.003$  W kg<sup>-1</sup> average negative power per side,  $1.244 \pm 0.400$  W kg<sup>-1</sup> peak power at  $15.0 \pm 1.2\%$  of the gait cycle, and  $0.476 \pm 0.087$  N·m kg<sup>-1</sup> peak moment at

14.9 ± 1.3% of the gait cycle. The force profile started at 10.0 ± 1.1% before heel strike and ended at 28.2 ± 1.5% after heel strike according to data from the treadmill physiological and biomechanical testing protocol (Fig. 2C). The running actuation profile resulted in 0.222 ± 0.055 W kg<sup>-1</sup> average positive power per side, -0.007 ± 0.008 W kg<sup>-1</sup> average negative power per side, 1.867 ± 0.465 W kg<sup>-1</sup> peak power at 21.1 ± 1.9% of the gait cycle, and 0.486 ± 0.076 N·m kg<sup>-1</sup> peak moment at 16.9 ± 1.7% of the gait cycle. The force profile started at 15.6 ± 2.7% before heel strike and ended at 31.0 ± 1.9% after heel strike. All the variabilities in the above walking and running actuation profiles are reported in standard deviations (SD).

An Atmel 32-bit microcontroller unit (MCU; ATSAME70N21, Atmel Corp., CA, USA) performs high-level controller computations at 1 kHz and communicates with the motor controllers and sensors. The 8-bit microprocessor units (PIC18F25K80, Microchip Technology, Inc., AZ, USA) attached to each IMU are used to read analog force signals from the load cell, as well as kinematic information (Euler angles, angular velocities, accelerations) for all three axes from the IMU, via a universal asynchronous receiver/transmitter (UART). To obtain a drift-free orientation estimate, each IMU is equipped with a built-in sensor fusion algorithm based on an extended Kalman filter. A controller area network (CAN) communication protocol is used for communication between the 8-bit MCUs, motor controllers, and the 32-bit MCU. In addition, the 32-bit MCU communicates with a telemetry laptop via a Bluetooth module (BT900-SC, Laird Technologies, UK) at 100 Hz for real-time data visualization with a graphical user interface, while simultaneously saving system data in the onboard flash memory card (SDSQUNC-032G-AN6IA, Scandisk, CA, USA) at 1 kHz. Both high-level algorithms and low-level firmware were programmed in standard C language (Visual Studio Code, Microsoft, WA, USA).

### Biologically inspired gait classification algorithm

Walking and running are often distinguished based on three different types of criteria: the presence or absence of flight phases (spatiotemporal criterion) (45), the extremum of knee flexion angle during mid-stance (kinematic criterion) (46), and the relative phase of the potential and kinetic energy of the CoM (dynamic criterion) (45). Walking has double-support phases, whereas running has flight phases. Determining if flight phases exist requires the accurate detection of heel-strike and toe-off events from each leg. However, it is challenging to catch these gait events robustly and reliably, especially for differentiating the presence or absence of very short flight phases, as this would require using foot-mounted sensors. Second, during the mid-stance phase, the knee is relatively straight during walking, but it is more flexed during running. However, measuring this knee flexion would require using IMU sensors on the shank in addition to the thigh. Lastly, potential and kinetic energy fluctuate out of phase during walking, whereas they fluctuate in phase during running. More specifically, the kinetic energy shows a similar pattern for both gaits, but the potential energy fluctuates differently for walking and running: at the time of heel strike, it is minimal for walking and maximal for running, which suggests that potential energy of the CoM could be used to distinguish walking and running gaits.

To minimize the system form factor and to avoid high metabolic penalty from distally added mass, we chose to differentiate walking and running by estimating potential energy using IMUs only on the proximal side of the body (47). We used the following

approximations: First, instead of estimating potential energy by measuring CoM height, we chose to base our classification algorithm on measuring vertical acceleration (in a global frame) to avoid drift-inducing errors when estimating distance with IMUs. Second, we estimated the location of the CoM with a single IMU. Measuring the exact location of the CoM requires the position and orientation of all body segments during the gait cycles, which would require multiple sets of sensors on all body segments. Among various sensor placement locations, we found that the abdomen was the best to approximate the movement of the CoM in preliminary testing. Third, since it is challenging to detect heel-strike events accurately using sensors worn above the knee joint, we used the maximum hip extension of the contralateral leg, which happens close to the heel strike, as the gait event to segment strides (Fig. 2A). By combining these three approximations, we selected the vertical acceleration of the abdomen IMU at the instant of maximum hip extension as a feature for distinguishing walking and running. At maximum hip extension, CoM potential energy is expected to be the local minimum for walking and local maximum for running; the vertical CoM acceleration, which is a twice-differentiated signal from CoM potential energy, is expected to be positive for walking and negative for running (Fig. 2B, movie S1).

Based on pilot testing, we confirmed that these approximations are valid. Since there is almost no overlap in the distributions of this feature for walking and running, a heuristic classifier can simply rely on thresholding feature value to classify each step as either walking or running gait. The algorithm switches between gait modes when a transition is detected for both legs. In theory, a threshold of  $0 \text{ m s}^{-2}$  could be used. However, we implemented a small tolerance margin that was maintained for all participants to increase reliability. To avoid false and frequent switching of the gait modes, the algorithm was designed to check that the feature is above (or below for walk-to-run transition) a given threshold for at least two consecutive steps before triggering a run-to-walk (or walk-to-run) transition. However, when the feature value changes from a strongly positive to a strongly negative value, or vice-versa, the controller allows a faster single-step-based transition. This strategy allows the algorithm to be sensitive enough to prevent uncomfortable actuation when transitioning between locomotion modes while ensuring increased robustness during steady-state locomotion.

#### Treadmill gait classification algorithm validation protocol

To evaluate the gait classification algorithm, we tested six male participants ( $28 \pm 3$  years;  $176.3 \pm 8.7$  cm;  $75.7 \pm 11.7$  kg, SD) during walking at three different speeds (1, 1.5 and  $2 \text{ m s}^{-1}$ ) and running at four different speeds (2, 2.5, 3 and  $3.5 \text{ m s}^{-1}$ ) on a treadmill (PPS MED, Woodway, WI, USA) at various grades (-10, -5, 0, 5, 10 and 15%). At a 20% slope, lower walking (1 and  $1.5 \text{ m s}^{-1}$ ) and running speeds ( $1.5$ , 2 and  $2.5 \text{ m s}^{-1}$ ) were tested, because the standard speeds were unfeasible at this slope. The order of the conditions was randomized. For each condition, we checked if the gait classification algorithm correctly identified walking and running. During the decline conditions, we only tested conditions up to  $2.5 \text{ m s}^{-1}$  due to the operating limits of the treadmill. For this evaluation, the system was worn but not actuated. Apart from the exosuit weight, no additional load was carried, and the participants wore their own running shoes. To evaluate the robustness of the algorithm for extreme cases, one additional test case was conducted: A randomly selected participant carried a 13.6 kg loaded backpack while wearing military boots for all of the aforementioned conditions, with additional  $0.5 \text{ m s}^{-1}$  walking and  $4.0 \text{ m s}^{-1}$  running

conditions. We recorded 40 steps per condition. The IMU signals and algorithm output were streamed at 100 Hz from the system to a telemetry laptop via Bluetooth.

#### Overground gait classification algorithm validation protocol

Eight males ( $28 \pm 2$  years;  $181.0 \pm 7.9$  cm;  $78.4 \pm 9.0$  kg, SD) participated in an overground testing protocol (fig. S3B, movie S2). Participants walked while wearing the exosuit with the assistance turned on (assist on), while wearing the exosuit with the assistance turned off (assist off), and without wearing the exosuit (no exo). The order of the three conditions was assigned randomly. Each condition consisted of four laps of 550 m for a total of 2.2 km per condition. The participants walked the first lap at  $1.5 \text{ m s}^{-1}$ , ran the next two laps at  $2.5 \text{ m s}^{-1}$ , and walked the final lap at  $1.5 \text{ m s}^{-1}$ . A researcher monitored the interval times every 110 m with a stopwatch and provided instructions to help the participant maintain the desired speed. Participants were allowed 10 minutes of rest between conditions. To evaluate the robustness of the classification algorithm, a researcher carrying a telemetry laptop manually recorded when a walk-to-run or run-to-walk transition was observed in the participant's gait. The first steps before and after the gait transition recorded by the experimenter were labeled transition periods and ignored in the gait classification accuracy evaluation. We also include the metabolic rate during the overground experiments using indirect calorimetry device (K4b2, Cosmed, Rome, Italy). These metabolic rate data were previously presented at a conference (28) and are provided in table S3. We calculated the metabolic rate based on  $\text{O}_2$  and  $\text{CO}_2$  data gathered from the last two minutes of each condition using the Brockway equation (48).

#### Treadmill physiological and biomechanical testing protocol

To evaluate the effects on biomechanics and metabolic rate, we tested nine male participants ( $28 \pm 5$  years;  $181.0 \pm 7.0$  cm;  $78.3 \pm 8.9$  kg, SD) while walking at  $1.5 \text{ m s}^{-1}$  and running at  $2.5 \text{ m s}^{-1}$  on a level treadmill (fig. S3A, movie S2). First, we measured the resting metabolic rate while participants stood still for 4 minutes. Then, the participants completed a warm-up consisting of 3 minutes of walking and 3 minutes of running. Participants then completed a combination of walking at  $1.5 \text{ m s}^{-1}$  and running at  $2.5 \text{ m s}^{-1}$  under the assist-on, assist-off, and no-exo conditions. The no-exo conditions were conducted at the beginning of the protocol and repeated a second time at the end of the protocol and the average was taken to avoid an order effect. All the other conditions were randomized. After the participants donned the exosuit, they completed two additional 5-minute adaptation periods of walking and running under the assist-on condition before the assist-on and assist-off conditions were tested. Each condition lasted 5 minutes, and participants were allowed at least a 3-minute break between conditions.

Indirect calorimetry (K4b2, Cosmed, Italy) was used to measure  $\text{O}_2$  consumption and  $\text{CO}_2$  production. Participants were asked to refrain from alcohol, caffeine and strenuous activities for twelve hours before the study and fast for two hours before the study. We calculated the metabolic rate based on  $\text{O}_2$  and  $\text{CO}_2$  data gathered from the last two minutes of each condition using the Brockway equation (48). We measured kinematics of the left leg using motion capture (Qualisys, Sweden) and reflective markers placed according to a Helen-Hayes-type marker set in seven ( $28 \pm 3$  years;  $181.3 \pm 8.0$  cm;  $78.7 \pm 9.8$  kg, SD) out of the nine participants. We measured ground reaction forces using an instrumented treadmill (Bertec, Columbus, OH, USA) at 2000 fps. We filtered motion capture data and

ground reaction force data using a 7-Hz or 15-Hz low-pass filter for walking or running, respectively. We calculated joint kinematics and internal joint moments and powers of the human plus the exosuit using rigid body mechanics in Visual3D (C-Motion, MD, USA). We calculated the external joint moment applied by the exosuit by multiplying the forces from the exosuit load cell with a moment arm of the force path of the Bowden cable relative to the hip joint calculated using motion capture. We calculated the external joint power applied by the exosuit by multiplying the exosuit moment by the hip joint angular velocity. We calculated the portion of the hip moment that is delivered by the biological muscles and passive tissues by subtracting the contribution of the exosuit from the total joint moment calculated by inverse dynamics. We measured activation of the left and right gluteus maximus, biceps femoris, rectus femoris, vastus lateralis, and the left gastrocnemius medialis, soleus, and tibialis muscles using surface electromyography (sEMG) at 2000 fps (Delsys, Natick, MA, USA). We processed sEMG data using a 20- to 450-Hz bandpass filter, rectification, and a 6-Hz low-pass filter. For each participant, we discarded parts of sEMG data based on visual inspection for artifacts due to sensor motion, sensor placement, sensor baseline drift and cable actuation (49). By default, we used sEMG data of the left leg for analysis, and we normalized sEMG based on the average of the two No Exo conditions. When artifacts were identified, we used sEMG data of the right leg (in 24.5% of all data), or we normalized sEMG data using only a single No Exo condition (in 22.4% of all data).

### Single-participant experiments

We conducted four single-participant experiments to evaluate the potential assistive effects and algorithm performance of the device under conditions other than those of the main protocol. To evaluate if the exosuit could reduce the metabolic rate during uphill walking, we tested one male participant (29 years; 167 cm; 60 kg) during walking on a 10% uphill treadmill at  $1.5 \text{ m s}^{-1}$ . To evaluate if the exosuit could reduce the metabolic rate during level running at different speeds, we tested the same participant running at 2.25, 2.5, 2.75, and  $3 \text{ m s}^{-1}$  on a treadmill. During both experiments, the participant walked or ran for 5 minutes in the assist-on and no-exo conditions. The conditions were randomized. An indirect calorimetry device (K5, Cosmed, Italy) was used to measure  $\text{O}_2$  consumption and  $\text{CO}_2$  production, and the metabolic rate was calculated based on the last two minutes of the data using the Brockway equation (48).

To evaluate the importance of the gait classification algorithm, the same participant performed a six-minute mixed walking and running condition, which consisted of three times one minute walking at  $1.5 \text{ m s}^{-1}$  and one minute running at  $2.5 \text{ m s}^{-1}$  in alternating order (thereby, three walk-to-run and two run-to-walk transitions). The participant completed this six-minute condition once with the correct actuation profiles, and once with the opposite actuation profiles (running actuation profile while walking, and vice versa while running). We measured  $\text{O}_2$  consumption and  $\text{CO}_2$  production and used the last two minutes of the data to calculate the metabolic rate using the Brockway equation (48).

To evaluate the potential effect of terrain on the classification algorithm performance we conducted a test on one male participant (23 years; 180 cm; 72 kg) at two outdoor locations (230- and 200-m paths) with uneven and unpaved terrain. We recorded separate bouts where the participant was walking (1.8 km in total), running (1.8 km in total), or performing gradual transitions between walking and running (0.8 km in total). An

experimenter carrying a telemetry laptop manually recorded the ground truth regarding when a walk-to-run or run-to-walk transition was observed in the participant's gait. During all single-participant experiments we measured kinematics from the IMU sensors (MTi-3 AHRS, Xsens Technologies B.V., Enschede, the Netherlands) and exosuit forces from the load cells (LSB200, FUTEK Advanced Sensor Technology, Inc., CA, USA).

### Participants

We used a convenience sampling strategy. For all protocols, we recruited participants who had previous experience with wearing the exosuit. The number of participants used for each protocol was based on similar studies in this field (11, 12, 23). We did not exclude participants. Participants were not blinded to the condition in which they were tested. All participants reported no previous history of musculoskeletal injury or other musculoskeletal diseases, and all participants provided written informed consent prior to participating in the study. We also obtained consent for publication of identifiable images in this manuscript. The study was approved by the Harvard Medical School Committee on Human Studies.

### Weight penalty estimation

To understand how the weights of the different components of the exosuit affected metabolic rate, we estimated the metabolic penalty by multiplying the added mass to each segment by coefficients reported in the literature for the effects of added mass during walking (25) and running (41, 50, 51). We evaluated how much of the difference between the assist-on and no-exo conditions would remain if the weight penalty would be exactly equal to the theoretical weight penalty from the literature (table S6).

### Statistics

We organized the data and conducted statistical analyses in MATLAB (MathWorks, Natick, MA, USA). For the classification algorithm protocols, we reported the classification feature in a histogram and calculated the number of true and false walking and running classifications. All other results are reported as the mean  $\pm$  standard error of the mean (SEM). The effects of the different conditions (assist-on, assist-off, and no-exo) on metabolic rate were analyzed using repeated measures ANOVA. If Mauchly's sphericity test was significant, we used the Greenhouse-Geisser corrected  $P$ -value. Differences between conditions were evaluated with paired  $t$  tests and the Holm-Šidák correction for multiple comparisons (52). For biomechanical parameters related to the effect of the assistance, we compared the assist-on and assist-off conditions using paired  $t$  tests. For parameters related to the effect of the weight and range of motion, we compared the assist-off versus no-exo condition using paired  $t$  tests. For all statistical tests that rely on the normality assumption, normality of the data was verified using the Jarque-Bera test. In one case where the normality assumption was not met, we used the Wilcoxon signed-rank test.

## Supplementary Text

### Challenge of assisting our evolutionarily optimized locomotor system

Through evolution, humans have become very skilled at walking and running (53). When moving slowly, we naturally prefer to walk at speeds (54) and step lengths (55) that minimize the metabolic cost of transport. We are remarkably good at distance running compared to other mammals thanks to long, spring-like tendons in the legs and hairless skin, which helps with thermoregulation. We spontaneously transition between walking and running at speeds that are close to the speed at which not switching gaits would be more metabolically expensive (56). It appears possible to reduce the metabolic rate of movements for which we are not evolutionarily optimized, such as assisting hopping in place with parallel leg springs (57) or assisting swimming with fins (58). Developing robotic assistive devices for walking and running is challenging not only because the biomechanics of both gaits are fundamentally different (4, 45, 59) but also because the biomechanics of both gaits have already been highly optimized through evolution. For example, robotic assistive devices that increase segment mass or alter the transition speed between walking and running from the optimal biological configuration could increase, rather than decrease, the metabolic rate.

### Benchmarks for reducing the metabolic rate with robotic assistive devices

In the previous decade, multiple incrementally challenging benchmarks have been considered for characterizing the performance of robotic assistive devices (60). To evaluate the assistive effects of a robotic assistive device independent of the penalty of wearing the passive structure, the metabolic rate of assisted locomotion is sometimes compared to that of locomotion while wearing the device with the assistance turned off. Comparison to the no-device baseline condition is a more stringent evaluation than comparison to a condition with the assistance turned off, because the positive effect of the assistance must be larger than the adverse effect of wearing the passive structure of the device to obtain a net positive result.

Much research has focused on developing lab-based and portable robotic assistive devices for reducing the metabolic rate of locomotion. Devices suitable for treadmill studies, i.e. with a nonportable power source tethered to the person have proven very useful for understanding wearer response to different actuation profiles. While very important to guide our basic scientific understanding, these treadmill type devices are limited to applications such as treadmill exercise therapy. Achieving a reduction in metabolic rate with a fully portable device requires careful attention to the design of compact and lightweight hardware as well as a control system that senses user intent using only device sensors. Fully autonomous systems are often tested on a treadmill to allow a more controlled testing environment. However, portable systems usually also enable overground and outdoor locomotion. Therefore, they can be used for applications involving mobility assistance in both healthy and impaired populations. A third class of robotic assistive devices are unpowered devices that rely exclusively on passive springs and clutches. Since these systems do not need actuators or batteries, they offer the additional advantage of unlimited autonomy. However, it remains to be understood whether these devices could reduce the metabolic rate of both walking and running since the elastic behavior of joints is different in both gaits (23, 61).

### Does switching between walking and running matter?

For slow speeds, walking is optimal, whereas for higher speeds, running is optimal (1, 2, 62). Metabolic rate measurements from studies on walking and running at different speeds indicate that at  $2.5 \text{ m s}^{-1}$ , walking is approximately 30% more metabolically expensive than running, and at  $1.5 \text{ m s}^{-1}$ , running is approximately twice as metabolically expensive as walking (63, 64). When the available time to cover a distance requires an average speed between 1.5 and  $4 \text{ m s}^{-1}$ , it is energetically favorable to use a combination of walking and running and transitions between both gaits rather than a single gait (65). This phenomenon is due to the nonconvex intersection of the metabolic rate landscapes of walking and running and explains why we spontaneously alternate between walking and running when trying to keep up with someone who walks faster than our comfortable speed. Furthermore, metabolic cost of transport landscapes shift with different terrain conditions, such as uphill and downhill grades. The optimal gait for a given speed can change depending on the grade (66).

It appears that the ability to switch between walking and running is important for minimizing energy consumption by selecting the optimal gait depending on changes in speed and terrain or even by allowing a combination of both gaits. A robotic assistive device that allows one to leverage this biological versatility can be advantageous for different professional groups such as soldiers, firefighters, and search-and-rescue teams (67). These professions often involve the need to move fast while carrying heavy loads (68) over terrain that requires switching between walking and running. Under such conditions, robotic assistive devices that are similar to the exosuit described here could potentially offset some part of the metabolic cost of carrying loads or allow the user to conserve more energy. Based on experience gained with the current system design, we expect that it would be possible to slightly further reduce the weight of the exosuit thereby making those practical applications more relevant.

In the present work, we show that it is possible to reduce the metabolic rate of walking and running through hip assistance by switching between actuation profiles for each gait. The single-participant experiment with the opposite actuation profiles demonstrates the importance of accurate gait classification and gait specific assistance. We found that applying the walking actuation profile during running and vice versa increases metabolic rate and variability in exosuit peak forces.

### Previous attempts at reducing the metabolic rate of walking and running

Early proposed solutions to allow both walking and running with a single robotic assistive device include quick-release connections that allow the rapid removal of a device (69) and a mode in which assistance becomes transparent (70). However, these solutions do not provide benefit during running.

Cherry et al. developed a full-lower-limb exoskeleton for assisting with running but found a 58% increase in the metabolic rate compared to running without the exoskeleton (13). A similar full-lower-limb running exoskeleton was developed by Hasegawa et al. (71), but no effects on the metabolic rate were reported. A variety of groups have evaluated full-lower-limb exoskeletons for walking, and the consensus appears to be that full-lower-limb exoskeletons are currently inadequate for reducing the metabolic rate of both walking and running due to their high mass and restrictive movement (72).

Elliott et al. developed a portable elastic knee exoskeleton with a clutch that was designed to assist running but resulted in a 27% increase in the metabolic rate compared to running without the exoskeleton (14). Knee exoskeletons have also been designed to assist walking (73) or to harvest electricity during walking (74). However, as far as we know, there have been no successful attempts to reduce the metabolic rate of walking with knee exoskeletons, possibly because the knee requires little positive work during walking. As such, studies of knee exoskeletons have not yet demonstrated their potential to reduce the metabolic rate of walking or running.

An early demonstration of reduced metabolic rate of walking was achieved with a tethered pneumatic ankle exoskeleton (75). More recently, Sovero et al. reported reductions in metabolic rate for three participants during running with an alternative design of a tethered pneumatic ankle exoskeleton (51). However, further work is required to create portable pneumatic systems that can reduce the metabolic rate of walking and running as well as operate over a long duration. Assisting walking and running has also been explored with tethered, electromechanically actuated ankle and hip exoskeletons. Zhang et al. developed a human-in-the-loop algorithm that allows for high reductions in the metabolic rate of walking and the same study showed that it is possible to reduce the metabolic rate of running in a single participant (76). It remains to be tested whether this type of actuation could be delivered by a portable system that can achieve the same metabolic results. In separate studies, our own group has previously reported metabolic reductions for walking (35) and running (27) with a tethered hip exosuit, where we used similar hardware but different assistance strategies.

In recent work with portable systems, Nasiri et al. reported reduction in the metabolic rate of running with an unpowered hip exoskeleton (23), and Lee et al. reported reduction in the metabolic rate of walking with a portable hip exoskeleton (17). As such, it seems that the hip joint is the only joint for which reductions in metabolic rate were achieved both during walking and running, although with different portable systems. We previously presented the metabolic rate of overground walking and running with the current exosuit at a conference (28). In that study, we found a significant reduction in the assist-on condition compared to the no-exo condition during overground running. We also found a reduction in the average metabolic rate in overground walking in assist-on compared to the no-exo condition, but this difference was not significant. Possible reasons for the absence of a significant reduction in metabolic rate in the overground walking condition of this previous study could be an issue with the sizing and fit of the exosuit components for one of the participants and the less strictly controlled conditions during overground testing compared to treadmill testing. We also found higher gait variability during the overground walking experiments (e.g. higher inter-stride standard deviation in IMU-based hip flexion angle,  $n = 7$ , two-sided paired  $t$  test,  $P = 0.030$ ) compared to that on the treadmill. An additional cause could be increased metabolic drift due to longer testing bouts in overground experiments and higher variability in ambient air conditions.

### Biomechanical explanation

We identified reductions in the hip and knee joint kinetics and activations of the surrounding muscles as potential explanations for the reductions in metabolic rate. The reductions in kinetics and activation at the hip joint were expected since the exosuit assists in parallel with the hip joint, and the reductions at the knee joint are consistent with

predictions from simulation studies and experimental studies with robotic assistive devices for the ankle that show it is possible to assist muscles that do not cross the joint actuated by the exoskeleton (24, 36, 77, 78). In addition, we found changes in other biomechanical parameters that do not immediately explain the reductions in metabolic rate (tables S4 and S5). Similar to other recent studies, we do not have a complete understanding of how the combined changes in biomechanical parameters explain the magnitude of the observed reductions in metabolic rate. Recent studies with human-in-the-loop optimization show that different individuals have different optimal actuation profiles (35, 76). Therefore, it is possible that reductions in metabolic rate come from different sources in different participants.

One basic way to interpret the relationship between the reduction in metabolic rate and the assistance provided is to calculate the apparent efficiency ratio of the bilateral sum of the positive work provided by the robotic assistive device divided by the reduction in metabolic rate in assist-on versus the assist-off condition. In our study, we found apparent efficiency ratios of  $0.487 \pm 0.556$  for walking and  $0.583 \pm 0.329$  for running (median  $\pm$  interquartile range, table S7). The results for both gaits fall within a range of apparent efficiency ratios found in previous studies examining walking with exoskeletons (0.61 in (10); 0.21 in (75)) and are not lower than the ratio that would be expected based on the apparent efficiency of biological muscles (79), which suggests that the observed reductions in metabolic rate are within an expected range.

A promising method to achieve a more comprehensive understanding of where the reductions in metabolic rate originate might be to conduct musculoskeletal simulations. In a recent study, Jackson et al. described a musculoskeletal model driven by muscle activation profiles and kinematics based on data from experiments with an exoskeleton. The model showed good agreement between measured biomechanical and physiological data (80). In conjunction with equations for calculating energy consumption from muscles (81), this type of simulation allows estimation of the metabolic energy consumption for different muscle groups and gait phases.

#### Possible future steps

While we chose to assist hip extension with an exosuit for the advantages of a low distal mass and unrestricted range of motion, this does not exclude the possibility of reducing the metabolic rate of walking and running by assisting other joints with other types of robotic assistive devices. The simulation studies by Uchida et al. (24) and Dembia et al. (77) provide an overview of the potential effects of assisting different degrees of freedom of different joints. According to these simulations, walking could be effectively assisted with devices that assist hip flexion, knee flexion or hip abduction, whereas for low speed running, assisting the ankle, the knee, or the hip appears to be approximately equally effective.

It may be possible to further reduce metabolic rate by making the actuation profiles adaptive based on certain parameters such as the gait speed. Studies regarding the biomechanics of walking and running show that changes in walking or running speed are associated with changes in magnitude and timing of hip extension moment and work (8, 82). It is possible that mimicking these changes in the exosuit actuation profiles could be beneficial. Furthermore, the simulation study presented by Uchida et al. (24) predicts that optimal hip actuation profiles are different for different speeds. Even though we did not

program an adaptation of the actuation profile to speed in the controller, the single-participant experiment that involved running at different speeds shows that the average positive power increases linearly from  $0.501 \pm 0.036$  (SD)  $\text{W kg}^{-1}$  at  $2.25 \text{ m s}^{-1}$  to  $0.774 \pm 0.050$  (SD)  $\text{W kg}^{-1}$  at  $3 \text{ m s}^{-1}$ . Nevertheless, it is possible that additional changes in the control algorithm could improve the assistance for walking and running at different speeds.

Recent studies have also shown that it can be highly beneficial to optimize actuation profiles specifically for every individual using an iterative process with real-time metabolic rate measurements, called human-in-the-loop optimization (35, 76, 83). It is likely that this method could also further improve the benefits of our exosuit for assisting walking and running. Improving the reduction in metabolic rate by increasing the peak force would require further development of textile components to ensure good user comfort at higher forces, in addition to careful analysis of the trade-off between the metabolic benefits of higher peak forces and the penalty of higher actuator weights required to achieve those peak forces.

Metabolic rate has been shown to be linearly correlated with performance times during long distance time-trials (44, 84). In this manuscript, we show that it is possible to improve the metabolic economy of walking and running at a fixed submaximal speed. Single-participant tests showed it is possible that the exosuit can reduce the metabolic rate of walking on a 10% grade and running at different speeds up to  $3 \text{ m s}^{-1}$  (Figs. 3D and 3E). An interesting follow-up study could consist of evaluating whether this improvement in metabolic economy could translate into increased walking and running speed during a maximal effort test, such as a time trial or graded exercise test.

Modified versions of this portable versatile exosuit could potentially also improve the mobility of clinical populations, such as elderly, stroke patients or patients with other cardiovascular or neurological diseases (85). It has been recently shown that a rigid hip exoskeleton that assists hip extension and hip flexion can reduce the metabolic rate of stair climbing in older adults (86). Stroke patients are known to have difficulty recruiting plantar flexor and hip flexor muscles at swing initiation (87). Our group recently conducted a small-scale, proof-of-concept study that demonstrated improved limb advancement in stroke patients using a tethered exosuit that assists hip flexion (88). In these patient populations, a potential advantage of an exosuit with an activity classification algorithm could be the ability to selectively assist certain actions but to otherwise have minimal impact on the individual.

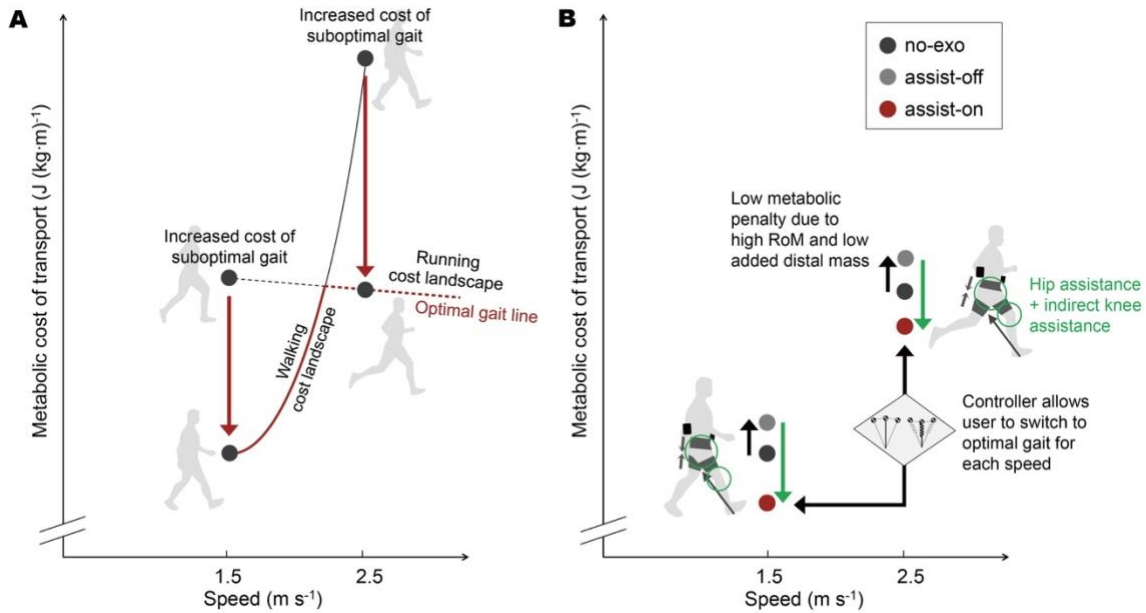


**Fig. S1. Schematic summary of the effects of the portable exosuit on walking and running.**

(A) The ability to switch to the optimal gait for each speed minimizes the metabolic cost of transport. Solid and dashed lines represent the metabolic cost of transport landscapes for walking and running, respectively (2). The part of the line that is marked in red represents the section where the gait selection is optimal. (B) The exosuit reduces the metabolic cost of transport by assisting hip extension and indirectly assisting knee extension. The benefit is not negated by the exosuit because of the low distal mass of the device and unrestricted range of motion. A controller that detects inverted pendulum or spring-mass behavior permits the wearer to switch between walking and running assistance.



**Fig. S2. Exosuit design.**

(A) Overall view of the system. (B) Base layer. (C) Actuator design. (D) Textile garment design. (E) Force transmission from motor to textile components. Textile component designs, a 3D visualization of the actuation system and a bill of materials are available in data S1, S2, and S6, respectively. Donning and doffing the exosuit is shown in movie S3.

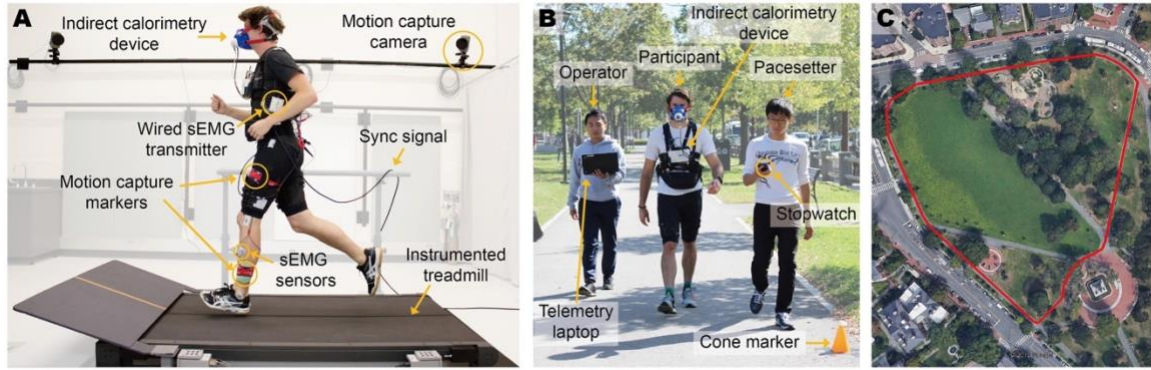


**Fig. S3. Experimental setup.**

(A) Treadmill physiological and biomechanical testing protocol. Participant running on a treadmill wearing the exosuit. A portable actuator generated hip extension forces. We measured exosuit forces using load cells, the metabolic rate using an indirect calorimetry device, kinematics using a motion capture system and IMUs, muscle activity using sEMG sensors, and ground reaction forces using a force-measuring treadmill. (B) Overground gait classification algorithm verification protocol. Participant walking outdoors with the exosuit over a flat and paved course. One researcher recorded data from the exosuit sensors with a telemetry laptop. Another researcher indicated the average pace that the participant must maintain. (C) Course map of the outdoor overground experiment (Cambridge Common, Cambridge, MA, USA). Red line represents a single lap (550 m) of the course. Videos of both protocols are in movie S2.

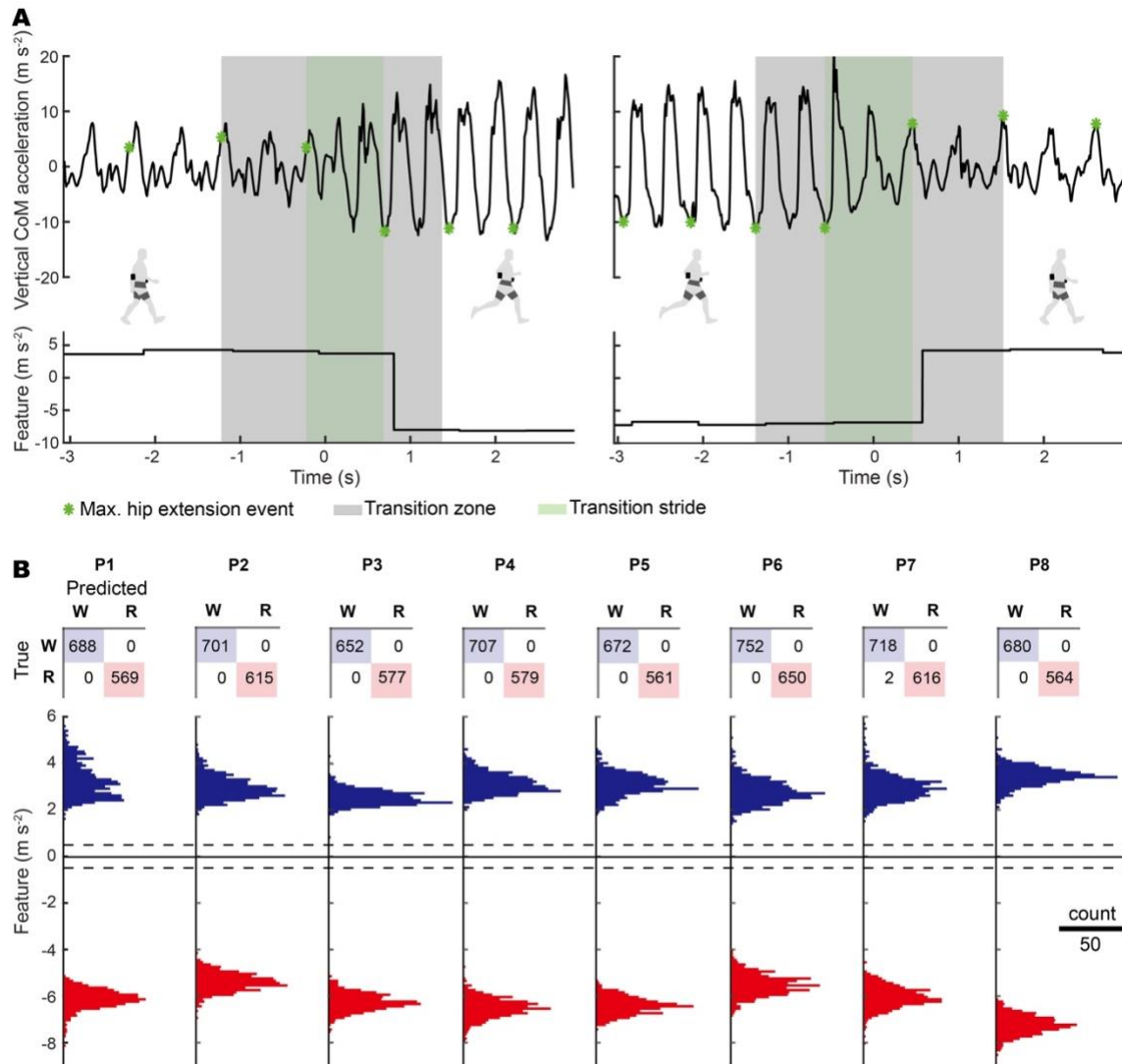


**Fig. S4. Overground gait classification experiment.**

(A) Vertical acceleration of the CoM and the feature extracted from the left leg during walk-to-run (left) and run-to-walk (right) transitions. (B) Distribution of the classification feature (vertical acceleration of the CoM at maximum hip extension (MHE)) and detailed classification results shown for each participant separately. Software code and source data are available in data S3 and S4.

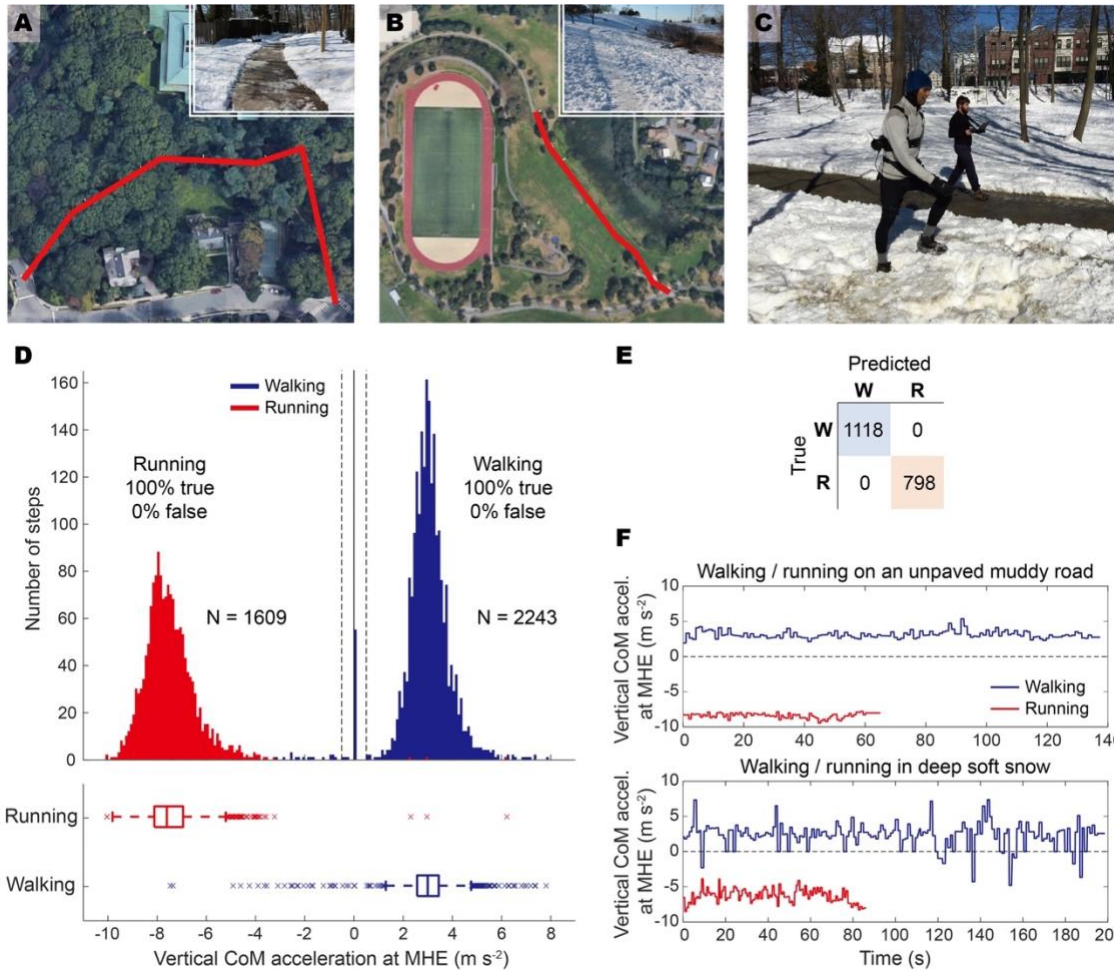


**Fig. S5. Single-participant outdoor overground testing on uneven terrain.**

(A) Map of a 230-m path (marked in red) at the American Academy of Arts & Sciences (Cambridge, MA, USA). Inset image shows an unpaved road with patches of snow and mud. (B) Map of a 200-m trail (marked in red) in Daney Park (Cambridge, MA, USA). Inset image shows an irregular icy trail with compacted snow. (C) Participant walking off-trail in deep (~20 cm) soft snow. (D) Histogram (top) and boxplot (bottom) of the classification feature (vertical CoM acceleration at maximum hip extension (MHE)) from both legs during uneven terrain test ( $n = 1$ ). The algorithm accuracy was 100%, despite unevenness of the ground surface or gradual changes in elevation. Additional filters (verifying if the threshold is crossed for two consecutive steps from both legs) prevented the algorithm from misclassifying gaits even when there were outliers in the feature that were larger than the threshold (data S3). (E) Algorithm accuracy for overall trials on uneven terrain ( $n = 1$ ). (F) The classification feature extracted from left leg over time while walking/running on an unpaved muddy road (top) and in deep soft snow (bottom). Larger deviations in the feature mostly came from walking/running off-trail in deep snow. In this trial, the participant's foot sank into the snow at every heel strike, which could cause altered vertical movement of body. Software code and source data are available in data S3 and S4.

**Table S1. Theoretical weight penalty calculation.**

Component mass for each segment, estimated penalty per kg of added mass for each segment, and the total estimated penalty for walking and running. When possible, we selected references with similar speeds and similar load-carrying setups (e.g., a belt or harness instead of a backpack). Penalty coefficients obtained from the literature were linearly rescaled according to the speeds used in our protocol.

		Bilateral added mass $m$ (g)	Metabolic penalty coefficients $\beta$ (W kg <sup>-1</sup> )	
			Walking at 1.5 m s <sup>-1</sup>	Running at 2.5 m s <sup>-1</sup>
<b>Waist</b>	Actuator	2674	4.005 (25)	5.737 (41)
	+ Load carrying belt with shoulder straps	363		
	+ Battery	1011		
	+ Battery bag	215		
	+ Waist belt	250		
	+ Abdomen IMU	29		
	Waist subtotal	4542		
<b>Thighs</b>	Thigh wraps	310	6.674 (25)	12.09 (51)
	+ Thigh IMUs and load cells	152		
	Thighs subtotal	462		
<b>Shanks</b>		0	6.763 (25)	29.57 (51)
<b>Feet</b>		0	17.80 (25)	42.26 (50)
<b>Expected metabolic penalty <math>\Sigma\beta_i m_i</math> (W)</b>			<b>21.27</b>	<b>31.64</b>

**Table S2. Net metabolic rate of treadmill protocol.**

\* indicates statistically significant difference for comparison versus the assist-on condition ( $n = 9$ , two-sided paired  $t$  test with Holm-Šidák correction,  $P < 0.05$ ). Source data are available in data S5.

Participant	Net metabolic rate ( $\text{W kg}^{-1}$ )					
	Treadmill walking at $1.5 \text{ m s}^{-1}$			Treadmill running at $2.5 \text{ m s}^{-1}$		
	assist off	no exo	assist on	assist off	no exo	assist on
1	3.305	2.829	2.521	10.117	9.813	9.001
2	4.490	4.177	3.674	11.442	10.943	10.364
3	4.479	4.348	4.387	10.714	10.534	10.445
4	4.920	4.436	4.188	11.267	10.670	10.147
5	3.563	3.324	2.822	9.773	9.528	9.294
6	3.845	3.879	3.380	11.308	11.105	10.118
7	4.577	4.448	4.321	12.181	11.928	11.604
8	4.841	3.920	3.610	12.233	11.725	10.998
9	4.345	4.406	3.553	10.478	10.020	10.441
<b>Mean <math>\pm</math> SEM</b>	<b>4.263</b> <b><math>\pm 0.188^*</math></b>	<b>3.974</b> <b><math>\pm 0.188^*</math></b>	<b>3.606</b> <b><math>\pm 0.214</math></b>	<b>11.057</b> <b><math>\pm 0.286^*</math></b>	<b>10.696</b> <b><math>\pm 0.275^*</math></b>	<b>10.268</b> <b><math>\pm 0.263</math></b>

**Table S3. Net metabolic rate of overground protocol.**

\* indicates statistically significant difference for comparison versus the assist-on condition ( $n = 8$ , two-sided paired  $t$  test with Holm-Šidák correction,  $P < 0.05$ ).

Participant	Net metabolic rate ( $\text{W kg}^{-1}$ )					
	Overground walking at $1.5 \text{ m s}^{-1}$			Overground running at $2.5 \text{ m s}^{-1}$		
	assist off	no exo	assist on	assist off	no exo	assist on
1	3.056	2.732	2.344	9.727	9.167	8.988
2	3.751	3.209	3.603	10.229	9.664	9.765
3	3.642	3.264	3.490	9.288	9.555	9.164
4	4.408	3.894	4.018	11.379	10.485	9.609
5	3.227	3.141	2.741	8.936	8.430	8.056
6	3.951	3.604	3.530	11.684	10.773	10.405
7	3.460	3.080	2.327	10.006	9.900	9.338
8	3.881	3.598	3.751	8.881	8.538	8.238
<b>Mean <math>\pm</math> SEM</b>	<b>3.672</b> <b><math>\pm 0.152^*</math></b>	<b>3.315</b> <b><math>\pm 0.129</math></b>	<b>3.226</b> <b><math>\pm 0.233</math></b>	<b>10.016</b> <b><math>\pm 0.372^*</math></b>	<b>9.564</b> <b><math>\pm 0.297^*</math></b>	<b>9.195</b> <b><math>\pm 0.275</math></b>

**Table S4. Treadmill protocol walking biomechanics.**

# and \* indicate statistical significance for the assist-off vs. no-exo and assist-on vs. assist-off comparisons, respectively ( $n = 7$ , two-sided paired  $t$  test,  $P < 0.05$ ). Source data are available in data S5.

		assist on	assist off	no exo	
		(Mean $\pm$ SEM)	(Mean $\pm$ SEM)	(Mean $\pm$ SEM)	
<b>Angle (<math>^{\circ}</math>)</b>					
Hip	Peak extension (+)	20.19 $\pm$ 1.95	17.86 $\pm$ 0.97	16.61 $\pm$ 1.23	#
	Peak flexion (-)	-22.25 $\pm$ 1.42	-23.09 $\pm$ 1.08	-26.33 $\pm$ 0.83	#
	Peak abduction (+)	5.40 $\pm$ 0.69	6.39 $\pm$ 0.96	6.81 $\pm$ 0.22	
	Peak adduction (-)	-7.24 $\pm$ 1.49	-7.60 $\pm$ 1.60	-6.22 $\pm$ 0.78	
	Peak external rotation (+)	7.98 $\pm$ 3.15	8.96 $\pm$ 3.01	6.01 $\pm$ 3.09	
	Peak internal rotation (-)	-2.51 $\pm$ 2.68	-1.47 $\pm$ 2.45	-4.51 $\pm$ 2.91	
	RoM in sagittal plane	42.44 $\pm$ 1.31	40.95 $\pm$ 1.76	42.94 $\pm$ 1.58	#
	RoM in coronal plane	12.64 $\pm$ 1.02	13.99 $\pm$ 0.95	13.03 $\pm$ 0.70	
Knee	RoM in transverse plane	10.49 $\pm$ 0.82	10.43 $\pm$ 1.02	10.52 $\pm$ 1.00	
	Peak extension (+)	-1.15 $\pm$ 2.65	-0.65 $\pm$ 2.39	0.04 $\pm$ 2.02	
	Peak flexion (-)	-74.24 $\pm$ 2.27	-74.08 $\pm$ 2.39	-72.59 $\pm$ 1.84	
	RoM in sagittal plane	73.09 $\pm$ 1.46	73.43 $\pm$ 1.53	72.62 $\pm$ 1.49	
Ankle	Peak plantar-flexion (+)	20.91 $\pm$ 1.55	24.08 $\pm$ 2.82	22.65 $\pm$ 1.58	
	Peak dorsi-flexion (-)	-13.49 $\pm$ 1.12	-13.10 $\pm$ 1.15	-12.03 $\pm$ 0.75	
	RoM in sagittal plane	34.40 $\pm$ 1.35	37.18 $\pm$ 2.32	34.68 $\pm$ 1.70	
<b>Moment (N·m kg<sup>-1</sup>)</b>					
Biological hip	Peak extension	0.757 $\pm$ 0.039	0.884 $\pm$ 0.046	0.832 $\pm$ 0.041	*
	Average extension	0.134 $\pm$ 0.007	0.166 $\pm$ 0.007	0.152 $\pm$ 0.009	*
	Peak flexion	-0.895 $\pm$ 0.082	-0.848 $\pm$ 0.086	-0.865 $\pm$ 0.089	
	Average flexion	-0.233 $\pm$ 0.025	-0.201 $\pm$ 0.020	-0.209 $\pm$ 0.023	*
Knee	Peak extension	0.950 $\pm$ 0.058	1.076 $\pm$ 0.069	1.032 $\pm$ 0.049	*
	Average extension	0.173 $\pm$ 0.007	0.190 $\pm$ 0.011	0.182 $\pm$ 0.006	
	Peak flexion	-0.515 $\pm$ 0.016	-0.493 $\pm$ 0.020	-0.508 $\pm$ 0.024	*
	Average flexion	-0.073 $\pm$ 0.005	-0.071 $\pm$ 0.005	-0.070 $\pm$ 0.004	
Ankle	Peak plantar-flexion	1.958 $\pm$ 0.055	1.971 $\pm$ 0.063	1.831 $\pm$ 0.069	
	Average plantar-flexion	0.460 $\pm$ 0.016	0.457 $\pm$ 0.023	0.426 $\pm$ 0.021	
	Peak dorsi-flexion	-0.217 $\pm$ 0.016	-0.234 $\pm$ 0.022	-0.225 $\pm$ 0.025	
	Average dorsi-flexion	-0.020 $\pm$ 0.001	-0.022 $\pm$ 0.002	-0.021 $\pm$ 0.002	
<b>Power (W kg<sup>-1</sup>)</b>					
Biological hip	Peak generation	1.375 $\pm$ 0.095	1.401 $\pm$ 0.123	1.442 $\pm$ 0.118	
	Average generation	0.308 $\pm$ 0.020	0.287 $\pm$ 0.025	0.284 $\pm$ 0.023	
	Peak absorption	-0.782 $\pm$ 0.133	-0.674 $\pm$ 0.075	-0.758 $\pm$ 0.075	
	Average absorption	-0.142 $\pm$ 0.025	-0.122 $\pm$ 0.016	-0.137 $\pm$ 0.021	
Knee	Peak generation	1.140 $\pm$ 0.114	1.198 $\pm$ 0.066	1.112 $\pm$ 0.087	
	Average generation	0.130 $\pm$ 0.008	0.153 $\pm$ 0.012	0.133 $\pm$ 0.009	*
	Peak absorption	-2.796 $\pm$ 0.138	-2.632 $\pm$ 0.104	-2.605 $\pm$ 0.167	
	Average absorption	-0.476 $\pm$ 0.011	-0.456 $\pm$ 0.020	-0.437 $\pm$ 0.015	
Ankle	Peak generation	5.120 $\pm$ 0.186	5.146 $\pm$ 0.235	4.739 $\pm$ 0.202	
	Average generation	0.381 $\pm$ 0.016	0.381 $\pm$ 0.019	0.357 $\pm$ 0.011	
	Peak absorption	-1.353 $\pm$ 0.055	-1.157 $\pm$ 0.060	-0.994 $\pm$ 0.082	
	Average absorption	-0.238 $\pm$ 0.004	-0.216 $\pm$ 0.007	-0.188 $\pm$ 0.008	*
<b>Normalized muscle activity (%)</b>					
Peak	Gluteus maximus	89.4 $\pm$ 4.9	104.2 $\pm$ 3.6	100.0 $\pm$ 0.0	*
	Biceps femoris	94.5 $\pm$ 5.1	94.3 $\pm$ 3.3	100.0 $\pm$ 0.0	
	Rectus femoris	100.9 $\pm$ 4.0	100.6 $\pm$ 5.6	100.0 $\pm$ 0.0	
	Vastus lateralis	83.9 $\pm$ 7.7	92.9 $\pm$ 5.0	100.0 $\pm$ 0.0	
	Gastrocnemius medialis	102.9 $\pm$ 4.0	107.8 $\pm$ 5.6	100.0 $\pm$ 0.0	*
	Soleus	104.3 $\pm$ 5.7	112.9 $\pm$ 8.6	100.0 $\pm$ 0.0	
	Tibialis anterior	103.2 $\pm$ 3.8	107.0 $\pm$ 2.3	100.0 $\pm$ 0.0	
	Average	Gluteus maximus	25.6 $\pm$ 2.2	28.2 $\pm$ 3.1	26.3 $\pm$ 2.1
Biceps femoris		25.1 $\pm$ 4.3	24.8 $\pm$ 5.1	24.8 $\pm$ 4.4	
Rectus femoris		28.6 $\pm$ 3.0	26.9 $\pm$ 2.3	26.7 $\pm$ 2.3	
Vastus lateralis		23.5 $\pm$ 1.7	23.3 $\pm$ 2.4	22.6 $\pm$ 1.6	
Gastrocnemius medialis		23.3 $\pm$ 1.7	23.1 $\pm$ 1.2	21.3 $\pm$ 0.8	
Soleus		30.4 $\pm$ 1.4	31.5 $\pm$ 0.8	28.5 $\pm$ 1.2	
Tibialis anterior		29.4 $\pm$ 2.3	29.2 $\pm$ 2.2	27.8 $\pm$ 1.9	
<b>Stride frequency (Hz)</b>					
		1.001 $\pm$ 0.015	0.971 $\pm$ 0.014	0.973 $\pm$ 0.016	*
<b>Duty factor (%)</b>					
		63.84 $\pm$ 0.40	63.11 $\pm$ 0.46	62.60 $\pm$ 0.54	*

**Table S5. Treadmill protocol running biomechanics.**

# and \* indicate statistical significance for the assist-off vs. no-exo and assist-on vs. assist-off comparisons, respectively ( $n = 7$ , two-sided paired  $t$  test,  $P < 0.05$ ). Source data are available in data S5.

		assist on	assist off	no exo	
		(Mean $\pm$ SEM)	(Mean $\pm$ SEM)	(Mean $\pm$ SEM)	
<b>Angle (<math>^{\circ}</math>)</b>					
Hip	Peak extension (+)	13.42 $\pm$ 2.12	12.57 $\pm$ 1.82	12.55 $\pm$ 2.21	
	Peak flexion (-)	-30.10 $\pm$ 1.97	-31.59 $\pm$ 1.45	-34.15 $\pm$ 2.04	
	Peak abduction (+)	5.62 $\pm$ 0.88	7.12 $\pm$ 0.98	7.59 $\pm$ 0.50	
	Peak adduction (-)	-9.49 $\pm$ 1.80	-9.23 $\pm$ 1.80	-11.03 $\pm$ 0.95	
	Peak external rotation (+)	8.70 $\pm$ 2.35	8.78 $\pm$ 2.07	5.54 $\pm$ 3.20	
	Peak internal rotation (-)	-3.71 $\pm$ 2.14	-4.31 $\pm$ 2.36	-7.87 $\pm$ 2.71	
	RoM in sagittal plane	43.52 $\pm$ 2.66	44.16 $\pm$ 2.53	46.69 $\pm$ 2.51	
	RoM in coronal plane	15.11 $\pm$ 1.61	16.35 $\pm$ 1.57	18.63 $\pm$ 1.35	#
Knee	RoM in transverse plane	12.41 $\pm$ 0.77	13.09 $\pm$ 1.48	13.41 $\pm$ 2.50	
	Peak extension (+)	-11.84 $\pm$ 1.89	-10.75 $\pm$ 1.96	-9.11 $\pm$ 1.67	
	Peak flexion (-)	-94.15 $\pm$ 7.00	-94.75 $\pm$ 6.76	-95.34 $\pm$ 6.14	
Ankle	RoM in sagittal plane	82.31 $\pm$ 6.18	84.01 $\pm$ 6.47	86.23 $\pm$ 5.52	
	Peak plantar-flexion (+)	24.89 $\pm$ 2.42	25.03 $\pm$ 2.30	27.37 $\pm$ 1.74	
	Peak dorsi-flexion (-)	-23.00 $\pm$ 0.91	-22.67 $\pm$ 0.97	-22.26 $\pm$ 0.93	
	RoM in sagittal plane	47.90 $\pm$ 2.31	47.69 $\pm$ 2.24	49.63 $\pm$ 1.84	#
<b>Moment (N·m kg<sup>-1</sup>)</b>					
Biological hip	Peak extension	1.197 $\pm$ 0.042	1.366 $\pm$ 0.062	1.325 $\pm$ 0.084	
	Average extension	0.232 $\pm$ 0.023	0.277 $\pm$ 0.023	0.248 $\pm$ 0.018	*
	Peak flexion	-0.908 $\pm$ 0.056	-0.894 $\pm$ 0.029	-0.859 $\pm$ 0.041	
	Average flexion	-0.272 $\pm$ 0.028	-0.250 $\pm$ 0.017	-0.246 $\pm$ 0.018	
Knee	Peak extension	2.900 $\pm$ 0.112	3.004 $\pm$ 0.110	2.787 $\pm$ 0.135	*
	Average extension	0.477 $\pm$ 0.015	0.486 $\pm$ 0.017	0.454 $\pm$ 0.016	
	Peak flexion	-0.628 $\pm$ 0.023	-0.638 $\pm$ 0.021	-0.638 $\pm$ 0.021	
Ankle	Average flexion	-0.095 $\pm$ 0.003	-0.098 $\pm$ 0.003	-0.099 $\pm$ 0.003	
	Peak plantar-flexion	2.990 $\pm$ 0.187	3.030 $\pm$ 0.213	2.912 $\pm$ 0.204	
	Average plantar-flexion	0.586 $\pm$ 0.040	0.580 $\pm$ 0.038	0.559 $\pm$ 0.040	
	Peak dorsi-flexion	-0.122 $\pm$ 0.037	-0.129 $\pm$ 0.036	-0.120 $\pm$ 0.026	
	Average dorsi-flexion	-0.013 $\pm$ 0.002	-0.014 $\pm$ 0.002	-0.013 $\pm$ 0.001	
<b>Power (W kg<sup>-1</sup>)</b>					
Biological hip	Peak generation	3.013 $\pm$ 0.402	3.449 $\pm$ 0.380	2.925 $\pm$ 0.335	
	Average generation	0.663 $\pm$ 0.080	0.743 $\pm$ 0.079	0.622 $\pm$ 0.087	*
	Peak absorption	-2.250 $\pm$ 0.547	-2.137 $\pm$ 0.205	-2.103 $\pm$ 0.250	
	Average absorption	-0.274 $\pm$ 0.090	-0.261 $\pm$ 0.043	-0.276 $\pm$ 0.043	
Knee	Peak generation	6.762 $\pm$ 0.517	6.477 $\pm$ 0.661	5.721 $\pm$ 0.704	
	Average generation	0.556 $\pm$ 0.038	0.578 $\pm$ 0.046	0.540 $\pm$ 0.053	
	Peak absorption	-11.385 $\pm$ 0.704	-11.175 $\pm$ 0.748	-11.164 $\pm$ 0.693	
Ankle	Average absorption	-1.462 $\pm$ 0.051	-1.469 $\pm$ 0.045	-1.392 $\pm$ 0.045	
	Peak generation	11.458 $\pm$ 1.291	11.493 $\pm$ 1.417	11.738 $\pm$ 1.382	
	Average generation	1.127 $\pm$ 0.097	1.128 $\pm$ 0.103	1.150 $\pm$ 0.108	
	Peak absorption	-7.143 $\pm$ 0.746	-7.402 $\pm$ 0.839	-7.316 $\pm$ 0.881	
	Average absorption	-0.810 $\pm$ 0.084	-0.803 $\pm$ 0.088	-0.801 $\pm$ 0.085	
<b>Normalized muscle activity (%)</b>					
Peak	Gluteus maximus	101.4 $\pm$ 12.6	97.3 $\pm$ 5.9	100.0 $\pm$ 0.0	
	Biceps femoris	100.8 $\pm$ 3.6	107.4 $\pm$ 3.8	100.0 $\pm$ 0.0	
	Rectus femoris	101.7 $\pm$ 6.9	104.9 $\pm$ 3.8	100.0 $\pm$ 0.0	
	Vastus lateralis	90.4 $\pm$ 4.2	95.6 $\pm$ 2.7	100.0 $\pm$ 0.0	
	Gastrocnemius medialis	96.8 $\pm$ 3.5	100.3 $\pm$ 2.0	100.0 $\pm$ 0.0	
	Soleus	96.7 $\pm$ 3.3	100.3 $\pm$ 2.3	100.0 $\pm$ 0.0	
	Tibialis anterior	119.9 $\pm$ 8.6	114.9 $\pm$ 9.3	100.0 $\pm$ 0.0	
	Average	Gluteus maximus	35.4 $\pm$ 4.4	34.1 $\pm$ 3.0	33.0 $\pm$ 1.4
Biceps femoris		25.5 $\pm$ 1.9	26.9 $\pm$ 1.6	25.6 $\pm$ 1.3	
Rectus femoris		29.8 $\pm$ 3.9	29.1 $\pm$ 3.7	28.2 $\pm$ 3.2	
Vastus lateralis		21.8 $\pm$ 1.2	21.3 $\pm$ 1.3	20.8 $\pm$ 1.1	
Gastrocnemius medialis		24.4 $\pm$ 2.4	24.1 $\pm$ 2.2	23.7 $\pm$ 2.0	
Soleus		26.6 $\pm$ 2.4	25.1 $\pm$ 1.2	24.5 $\pm$ 1.2	
Tibialis anterior		48.9 $\pm$ 6.6	46.2 $\pm$ 6.9	42.0 $\pm$ 4.4	
<b>Stride frequency (Hz)</b>					
		1.344 $\pm$ 0.028	1.348 $\pm$ 0.034	1.315 $\pm$ 0.032	
<b>Duty factor (%)</b>					
		40.39 $\pm$ 1.55	39.37 $\pm$ 1.48	38.43 $\pm$ 1.37	

**Table S6. Verification of metabolic rate reduction assuming theoretical weight penalty.**

Based on data from treadmill protocol. We estimated what the metabolic rate in the assist-on condition would be if the weight penalty was equal to the theoretical weight penalty from table S1. In order to obtain weight penalty adjusted metabolic rate of the assist-on condition, we added the theoretical weight penalty and the difference between assist-on and assist-off to the metabolic rate of the no-exo condition, with the assumption that the metabolic rate difference between assist-on and assist-off still remains unchanged. \* indicates statistically significant difference ( $n = 9$ , two-sided paired  $t$  test with Holm-Šidák correction,  $P < 0.05$ ).

	<b>Walking</b> (mean $\pm$ SEM)	<b>Running</b> (mean $\pm$ SEM)
Measured metabolic rate in the assist-on condition ( $W \text{ kg}^{-1}$ )	3.606 $\pm$ 0.214	10.268 $\pm$ 0.263
Measured reduction in assist-on versus no-exo (%)	9.3 $\pm$ 2.2 *	4.0 $\pm$ 1.3 *
Theoretical weight penalty in no-exo versus assist-off ( $W \text{ kg}^{-1}$ )	0.275 $\pm$ 0.012	0.409 $\pm$ 0.017
Weight penalty adjusted metabolic rate of the assist-on condition ( $W \text{ kg}^{-1}$ )	3.593 $\pm$ 0.252	10.316 $\pm$ 0.264
Adjusted metabolic rate reduction in assist-on versus no-exo (%)	9.6 $\pm$ 2.8 *	3.6 $\pm$ 1.3 *

**Table S7. Apparent efficiency ratio of average positive power versus change in metabolic rate.**

Based on biomechanical and metabolic rate data for participants evaluated on the treadmill protocol ( $n = 7$ ).

	<b>Walking</b>	<b>Running</b>
Bilateral sum of average positive power from exosuit (W kg <sup>-1</sup> ) (mean $\pm$ SEM)	0.250 $\pm$ 0.029	0.443 $\pm$ 0.041
Reduction in metabolic rate between assist-on and assist-off (W kg <sup>-1</sup> ) (mean $\pm$ SEM)	0.555 $\pm$ 0.109	0.833 $\pm$ 0.143
Apparent efficiency ratio of mechanical work divided by change in metabolic rate (median $\pm$ interquartile range)	0.487 $\pm$ 0.556	0.583 $\pm$ 0.329

**Movie S1. Demonstration of exosuit during walking and running in the treadmill and overground outdoor settings.**

The first part of the movie shows the actuator pulling the cable to apply force and pushing out the cable to allow unrestricted motion during the swing phase. The second part of the movie shows the measurement of the CoM vertical acceleration at maximum hip extension, a gradual transition between running and walking, and how this is used to control the appropriate switch in actuation profile. The last part of the video shows how the device works during overground walking and running.

**Movie S2. Description of the experimental setup.**

The first part of this video shows the treadmill physiological and biomechanical testing protocol. We measured exosuit forces using load cells, the metabolic rate using an indirect calorimetry device, kinematics using a motion capture system and IMUs, muscle activity using surface electromyography (sEMG) sensors, and ground reaction forces using an instrumented treadmill. The last part of this video shows the overground gait classification algorithm validation protocol. The participant wore the exosuit and an indirect calorimetry unit. One researcher recorded data from the exosuit sensors with a telemetry laptop. Another researcher indicated the average pace that the participant must maintain.

**Movie S3. Exosuit donning and doffing.**

This first part of this video shows one participant donning the shoulder straps followed by the waist belt and thigh wraps in 1 minute 46 seconds. The second part shows the participant doffing the exosuit in 31 seconds.

**Data S1. Textile-component designs.**

Schematics of the waist belt and thigh wrap construction.

**Data S2. 3D visualization of actuation system.**

Actuation unit, Bowden cables, fasteners, and load cells.

**Data S3. Software code.**

A pseudocode description of different sub-algorithms: gait cycle events detection, gait classifier, and motor position trajectory design.

**Data S4. Gait classification algorithm data.**

Data file contains deidentified preprocessed individual time series and metrics of the gait classification experiments (Treadmill gait classification algorithm validation protocol, Overground gait classification algorithm validation protocol, Treadmill physiological and biomechanical testing protocol, and single-participant experiments).

**Data S5. Biomechanical testing data.**

Data file contains deidentified preprocessed individual time series and metrics of the treadmill physiological and biomechanical testing protocol.

**Data S6. Bill of materials.**

Description, quantity, part numbers and manufacturer information for the materials of the exosuit.

## References and Notes

1. R. Margaria, P. Cerretelli, P. Aghemo, G. Sassi, Energy cost of running. *J. Appl. Physiol.* **18**, 367–370 (1963). [doi:10.1152/jappl.1963.18.2.367](https://doi.org/10.1152/jappl.1963.18.2.367) [Medline](#)
2. D. R. Carrier, A. K. Kapoor, T. Kimura, M. K. Nickels, E. C. Scott, J. K. So, E. Trinkaus, The Energetic Paradox of Human Running and Hominid Evolution. *Curr. Anthropol.* **25**, 483–495 (1984). [doi:10.1086/203165](https://doi.org/10.1086/203165)
3. Materials and methods, supplementary text, figures, tables, movies, and datasets are available as supplementary materials.
4. G. A. Cavagna, M. Kaneko, Mechanical work and efficiency in level walking and running. *J. Physiol.* **268**, 467–481 (1977). [doi:10.1113/jphysiol.1977.sp011866](https://doi.org/10.1113/jphysiol.1977.sp011866) [Medline](#)
5. T. A. McMahon, G. Valiant, E. C. Frederick, Groucho running. *J. Appl. Physiol.* **62**, 2326–2337 (1987). [doi:10.1152/jappl.1987.62.6.2326](https://doi.org/10.1152/jappl.1987.62.6.2326) [Medline](#)
6. T. A. McMahon, G. C. Cheng, The mechanics of running: How does stiffness couple with speed? *J. Biomech.* **23** (Suppl 1), 65–78 (1990). [doi:10.1016/0021-9290\(90\)90042-2](https://doi.org/10.1016/0021-9290(90)90042-2) [Medline](#)
7. R. M. Alexander, *The Spring in Your Step: The Role of Elastic Mechanisms in Human Running*, vol. XI-A (Free University Press, 1988).
8. A. G. Schache, P. D. Blanch, T. W. Dorn, N. A. T. Brown, D. Rosemond, M. G. Pandy, Effect of running speed on lower limb joint kinetics. *Med. Sci. Sports Exerc.* **43**, 1260–1271 (2011). [doi:10.1249/MSS.0b013e3182084929](https://doi.org/10.1249/MSS.0b013e3182084929) [Medline](#)
9. D. J. Farris, G. S. Sawicki, The mechanics and energetics of human walking and running: A joint level perspective. *J. R. Soc. Interface* **9**, 110–118 (2011). [doi:10.1098/rsif.2011.0182](https://doi.org/10.1098/rsif.2011.0182) [Medline](#)
10. G. S. Sawicki, D. P. Ferris, Mechanics and energetics of level walking with powered ankle exoskeletons. *J. Exp. Biol.* **211**, 1402–1413 (2008). [doi:10.1242/jeb.009241](https://doi.org/10.1242/jeb.009241) [Medline](#)
11. L. M. Mooney, E. J. Rouse, H. M. Herr, Autonomous exoskeleton reduces metabolic cost of human walking during load carriage. *J. Neuroeng. Rehabil.* **11**, 80 (2014). [doi:10.1186/1743-0003-11-80](https://doi.org/10.1186/1743-0003-11-80) [Medline](#)
12. S. H. Collins, M. B. Wiggin, G. S. Sawicki, Reducing the energy cost of human walking using an unpowered exoskeleton. *Nature* **522**, 212–215 (2015). [doi:10.1038/nature14288](https://doi.org/10.1038/nature14288) [Medline](#)
13. M. S. Cherry, S. Kota, A. Young, D. P. Ferris, Running with an elastic lower limb exoskeleton. *J. Appl. Biomech.* **32**, 269–277 (2016). [doi:10.1123/jab.2015-0155](https://doi.org/10.1123/jab.2015-0155) [Medline](#)
14. G. Elliott, G. S. Sawicki, A. Marecki, H. Herr, in *2013 IEEE 13th International Conference on Rehabilitation Robotics* (IEEE, 2013), document 6650418.
15. C. S. Simpson, C. G. Welker, S. D. Uhlrich, S. M. Sketch, R. W. Jackson, S. L. Delp, S. H. Collins, J. C. Selinger, E. W. Hawkes, Connecting the legs with a spring improves human running economy. bioRxiv 474650 [Preprint]. 30 November 2018. <https://doi.org/10.1101/474650>.

16. S. Lee, J. Kim, L. Baker, A. Long, N. Karavas, N. Menard, I. Galiana, C. J. Walsh, Autonomous multi-joint soft exosuit with augmentation-power-based control parameter tuning reduces energy cost of loaded walking. *J. Neuroeng. Rehabil.* **15**, 66 (2018). [doi:10.1186/s12984-018-0410-y](https://doi.org/10.1186/s12984-018-0410-y) [Medline](#)
17. J. Lee, K. Seo, B. Lim, J. Jang, K. Kim, H. Choi, Effects of assistance timing on metabolic cost, assistance power, and gait parameters for a hip-type exoskeleton. *IEEE Int. Conf. Rehabil. Robot.* **2017**, 498–504 (2017). [Medline](#)
18. C. R. Taylor, N. C. Heglund, T. A. McMahon, T. R. Looney, Energetic cost of generating muscular force during running: A comparison of large and small animals. *J. Exp. Biol.* **86**, 9–18 (1980).
19. G. M. O. Maloiy, N. C. Heglund, L. M. Prager, G. A. Cavagna, C. R. Taylor, Energetic cost of carrying loads: Have African women discovered an economic way? *Nature* **319**, 668–669 (1986). [doi:10.1038/319668a0](https://doi.org/10.1038/319668a0) [Medline](#)
20. T. M. Griffin, T. J. Roberts, R. Kram, Metabolic cost of generating muscular force in human walking: Insights from load-carrying and speed experiments. *J. Appl. Physiol.* **95**, 172–183 (2003). [doi:10.1152/jappphysiol.00944.2002](https://doi.org/10.1152/jappphysiol.00944.2002) [Medline](#)
21. E. C. Frederick, Physiological and ergonomics factors in running shoe design. *Appl. Ergon.* **15**, 281–287 (1984). [doi:10.1016/0003-6870\(84\)90199-6](https://doi.org/10.1016/0003-6870(84)90199-6) [Medline](#)
22. M. J. Myers, K. Steudel, Effect of limb mass and its distribution on the energetic cost of running. *J. Exp. Biol.* **116**, 363–373 (1985). [Medline](#)
23. R. Nasiri, A. Ahmadi, M. N. Ahmadabadi, Reducing the energy cost of human running using an unpowered exoskeleton. *IEEE Trans. Neural Syst. Rehabil. Eng.* **26**, 2026–2032 (2018). [doi:10.1109/TNSRE.2018.2872889](https://doi.org/10.1109/TNSRE.2018.2872889) [Medline](#)
24. T. K. Uchida, A. Seth, S. Pouya, C. L. Dembia, J. L. Hicks, S. L. Delp, Simulating ideal assistive devices to reduce the metabolic cost of running. *PLOS ONE* **11**, e0163417 (2016). [doi:10.1371/journal.pone.0163417](https://doi.org/10.1371/journal.pone.0163417) [Medline](#)
25. R. C. Browning, J. R. Modica, R. Kram, A. Goswami, The effects of adding mass to the legs on the energetics and biomechanics of walking. *Med. Sci. Sports Exerc.* **39**, 515–525 (2007). [doi:10.1249/mss.0b013e31802b3562](https://doi.org/10.1249/mss.0b013e31802b3562) [Medline](#)
26. Y. Ding, F. A. Panizzolo, C. Siviyy, P. Malcolm, I. Galiana, K. G. Holt, C. J. Walsh, Effect of timing of hip extension assistance during loaded walking with a soft exosuit. *J. Neuroeng. Rehabil.* **13**, 87 (2016). [doi:10.1186/s12984-016-0196-8](https://doi.org/10.1186/s12984-016-0196-8) [Medline](#)
27. G. Lee, J. Kim, F. A. Panizzolo, Y. M. Zhou, L. M. Baker, I. Galiana, P. Malcolm, C. J. Walsh, Reducing the metabolic cost of running with a tethered soft exosuit. *Sci. Robot.* **2**, eaan6708 (2017). [doi:10.1126/scirobotics.aan6708](https://doi.org/10.1126/scirobotics.aan6708)
28. J. Kim *et al.*, Autonomous and portable soft exosuit for hip extension assistance with online walking and running detection algorithm. *ICRA*, 5473–5480 (2018).
29. A. S. Voloshina, D. P. Ferris, Biomechanics and energetics of running on uneven terrain. *J. Exp. Biol.* **218**, 711–719 (2015). [doi:10.1242/jeb.106518](https://doi.org/10.1242/jeb.106518) [Medline](#)

30. A. S. Voloshina, A. D. Kuo, M. A. Daley, D. P. Ferris, Biomechanics and energetics of walking on uneven terrain. *J. Exp. Biol.* **216**, 3963–3970 (2013). [doi:10.1242/jeb.081711](https://doi.org/10.1242/jeb.081711) [Medline](#)
31. S. J. Preece, J. Y. Goulermas, L. P. J. Kenney, D. Howard, K. Meijer, R. Crompton, Activity identification using body-mounted sensors—A review of classification techniques. *Physiol. Meas.* **30**, R1–R33 (2009). [doi:10.1088/0967-3334/30/4/R01](https://doi.org/10.1088/0967-3334/30/4/R01) [Medline](#)
32. A. H. Shultz, B. E. Lawson, M. Goldfarb, Running with a powered knee and ankle prosthesis. *IEEE Trans. Neural Syst. Rehabil. Eng.* **23**, 403–412 (2015). [Medline](#)
33. J. R. Koller, D. A. Jacobs, D. P. Ferris, C. D. Remy, Learning to walk with an adaptive gain proportional myoelectric controller for a robotic ankle exoskeleton. *J. Neuroeng. Rehabil.* **12**, 97 (2015). [doi:10.1186/s12984-015-0086-5](https://doi.org/10.1186/s12984-015-0086-5) [Medline](#)
34. B. Wiggin, thesis, North Carolina State University (2014).
35. Y. Ding, M. Kim, S. Kuindersma, C. J. Walsh, Human-in-the-loop optimization of hip assistance with a soft exosuit during walking. *Sci. Robot.* **3**, eaar5438 (2018). [doi:10.1126/scirobotics.aar5438](https://doi.org/10.1126/scirobotics.aar5438)
36. L. M. Mooney, H. M. Herr, Biomechanical walking mechanisms underlying the metabolic reduction caused by an autonomous exoskeleton. *J. Neuroeng. Rehabil.* **13**, 4 (2016). [doi:10.1186/s12984-016-0111-3](https://doi.org/10.1186/s12984-016-0111-3) [Medline](#)
37. T. S. Bae, K. Choi, D. Hong, M. Mun, Dynamic analysis of above-knee amputee gait. *Clin. Biomech.* **22**, 557–566 (2007). [doi:10.1016/j.clinbiomech.2006.12.009](https://doi.org/10.1016/j.clinbiomech.2006.12.009) [Medline](#)
38. B. R. Umberger, P. E. Martin, Mechanical power and efficiency of level walking with different stride rates. *J. Exp. Biol.* **210**, 3255–3265 (2007). [doi:10.1242/jeb.000950](https://doi.org/10.1242/jeb.000950) [Medline](#)
39. J. Doke, J. M. Donelan, A. D. Kuo, Mechanics and energetics of swinging the human leg. *J. Exp. Biol.* **208**, 439–445 (2005). [doi:10.1242/jeb.01408](https://doi.org/10.1242/jeb.01408) [Medline](#)
40. G. O. Dahlbäck, R. Norlin, The effect of corrective surgery on energy expenditure during ambulation in children with cerebral palsy. *Eur. J. Appl. Physiol. Occup. Physiol.* **54**, 67–70 (1985). [doi:10.1007/BF00426301](https://doi.org/10.1007/BF00426301) [Medline](#)
41. K. J. Cureton, P. B. Sparling, B. W. Evans, S. M. Johnson, U. D. Kong, J. W. Purvis, Effect of experimental alterations in excess weight on aerobic capacity and distance running performance. *Med. Sci. Sports* **10**, 194–199 (1978). [Medline](#)
42. W. Hoogkamer, S. Kipp, J. H. Frank, E. M. Farina, G. Luo, R. Kram, A Comparison of the Energetic Cost of Running in Marathon Racing Shoes. *Sports Med.* **48**, 1009–1019 (2017). [doi:10.1007/s40279-017-0811-2](https://doi.org/10.1007/s40279-017-0811-2) [Medline](#)
43. S. Galle, P. Malcolm, W. Derave, D. De Clercq, Enhancing performance during inclined loaded walking with a powered ankle-foot exoskeleton. *Eur. J. Appl. Physiol.* **114**, 2341–2351 (2014). [doi:10.1007/s00421-014-2955-1](https://doi.org/10.1007/s00421-014-2955-1) [Medline](#)
44. W. Hoogkamer, S. Kipp, B. A. Spiering, R. Kram, Altered running economy directly translates to altered distance-running performance. *Med. Sci. Sports Exerc.* **48**, 2175–2180 (2016). [doi:10.1249/MSS.0000000000001012](https://doi.org/10.1249/MSS.0000000000001012) [Medline](#)

45. C. T. Farley, D. P. Ferris, Biomechanics of walking and running: Center of mass movements to muscle action. *Exerc. Sport Sci. Rev.* **26**, 253–285 (1998). [Medline](#)
46. T. F. Novacheck, The biomechanics of running. *Gait Posture* **7**, 77–95 (1998). [doi:10.1016/S0966-6362\(97\)00038-6](https://doi.org/10.1016/S0966-6362(97)00038-6) [Medline](#)
47. S. A. Gard, S. C. Miff, A. D. Kuo, Comparison of kinematic and kinetic methods for computing the vertical motion of the body center of mass during walking. *Hum. Mov. Sci.* **22**, 597–610 (2004). [doi:10.1016/j.humov.2003.11.002](https://doi.org/10.1016/j.humov.2003.11.002) [Medline](#)
48. J. M. Brockway, Derivation of formulae used to calculate energy expenditure in man. *Hum. Nutr. Clin. Nutr.* **41**, 463–471 (1987). [Medline](#)
49. R. W. Jackson, S. H. Collins, An experimental comparison of the relative benefits of work and torque assistance in ankle exoskeletons. *J. Appl. Physiol.* **119**, 541–557 (2015). [doi:10.1152/jappphysiol.01133.2014](https://doi.org/10.1152/jappphysiol.01133.2014) [Medline](#)
50. J. R. Franz, C. M. Wierzbinski, R. Kram, Metabolic cost of running barefoot versus shod: Is lighter better? *Med. Sci. Sports Exerc.* **44**, 1519–1525 (2012). [doi:10.1249/MSS.0b013e3182514a88](https://doi.org/10.1249/MSS.0b013e3182514a88) [Medline](#)
51. S. Sovero *et al.*, “Initial Data and Theory for a High Specific-Power Ankle Exoskeleton Device” in *2016 International Symposium on Experimental Robotics*, (Springer Proceedings in Advanced Robotics Series, Springer, 2017), pp. 355–364.
52. S. A. Glantz, *Primer of Biostatistics* (McGraw-Hill Medical, ed. 6, 2005).
53. R. M. Alexander, *Principles of Animal Locomotion* (Princeton Univ. Press, 2003).
54. H. J. Ralston, Energy-speed relation and optimal speed during level walking. *Int. Z. Angew. Physiol.* **17**, 277–283 (1958). [Medline](#)
55. M. Y. Zarrugh, F. N. Todd, H. J. Ralston, Optimization of energy expenditure during level walking. *Eur. J. Appl. Physiol. Occup. Physiol.* **33**, 293–306 (1974). [doi:10.1007/BF00430237](https://doi.org/10.1007/BF00430237) [Medline](#)
56. A. Hreljac, Preferred and energetically optimal gait transition speeds in human locomotion. *Med. Sci. Sports Exerc.* **25**, 1158–1162 (1993). [doi:10.1249/00005768-199310000-00012](https://doi.org/10.1249/00005768-199310000-00012) [Medline](#)
57. A. M. Grabowski, H. M. Herr, Leg exoskeleton reduces the metabolic cost of human hopping. *J. Appl. Physiol.* **107**, 670–678 (2009). [doi:10.1152/jappphysiol.91609.2008](https://doi.org/10.1152/jappphysiol.91609.2008) [Medline](#)
58. P. Zamparo, D. R. Pendergast, B. Termin, A. E. Minetti, How fins affect the economy and efficiency of human swimming. *J. Exp. Biol.* **205**, 2665–2676 (2002). [Medline](#)
59. G. A. Cavagna, N. C. Heglund, C. R. Taylor, Mechanical work in terrestrial locomotion: Two basic mechanisms for minimizing energy expenditure. *Am. J. Physiol.* **233**, R243–R261 (1977). [Medline](#)
60. D. Torricelli, J. Gonzalez-Vargas, J. F. Veneman, K. Mombaur, N. Tsagarakis, A. J. del-Ama, A. Gil-Agudo, J. C. Moreno, J. L. Pons, Benchmarking Bipedal Locomotion: A Unified Scheme for Humanoids, Wearable Robots, and Humans. *IEEE Robot. Autom. Mag.* **22**, 103–115 (2015). [doi:10.1109/MRA.2015.2448278](https://doi.org/10.1109/MRA.2015.2448278)

61. G. A. Lichtwark, A. M. Wilson, Optimal muscle fascicle length and tendon stiffness for maximising gastrocnemius efficiency during human walking and running. *J. Theor. Biol.* **252**, 662–673 (2008). [doi:10.1016/j.jtbi.2008.01.018](https://doi.org/10.1016/j.jtbi.2008.01.018) [Medline](#)
62. D. F. Hoyt, C. R. Taylor, Gait and the energetics of locomotion in horses. *Nature* **292**, 239–240 (1981). [doi:10.1038/292239a0](https://doi.org/10.1038/292239a0)
63. Y. Epstein, L. A. Stroschein, K. B. Pandolf, Predicting metabolic cost of running with and without backpack loads. *Eur. J. Appl. Physiol. Occup. Physiol.* **56**, 495–500 (1987). [doi:10.1007/BF00635360](https://doi.org/10.1007/BF00635360) [Medline](#)
64. K. B. Pandolf, B. Givoni, R. F. Goldman, Predicting energy expenditure with loads while standing or walking very slowly. *J. Appl. Physiol.* **43**, 577–581 (1977). [doi:10.1152/jappl.1977.43.4.577](https://doi.org/10.1152/jappl.1977.43.4.577) [Medline](#)
65. L. L. Long 3rd, M. Srinivasan, Walking, running, and resting under time, distance, and average speed constraints: Optimality of walk-run-rest mixtures. *J. R. Soc. Interface* **10**, 20120980 (2013). [doi:10.1098/rsif.2012.0980](https://doi.org/10.1098/rsif.2012.0980) [Medline](#)
66. A. E. Minetti, L. P. Ardigò, F. Saibene, The transition between walking and running in humans: Metabolic and mechanical aspects at different gradients. *Acta Physiol. Scand.* **150**, 315–323 (1994). [doi:10.1111/j.1748-1716.1994.tb09692.x](https://doi.org/10.1111/j.1748-1716.1994.tb09692.x) [Medline](#)
67. R. Bogue, Robotic exoskeletons: A review of recent progress. *Ind. Rob.* **42**, 5–10 (2015). [doi:10.1108/IR-08-2014-0379](https://doi.org/10.1108/IR-08-2014-0379)
68. J. J. Knapik, K. L. Reynolds, E. Harman, Soldier load carriage: Historical, physiological, biomechanical, and medical aspects. *Mil. Med.* **169**, 45–56 (2004). [doi:10.7205/MILMED.169.1.45](https://doi.org/10.7205/MILMED.169.1.45) [Medline](#)
69. A. B. Zoss, H. Kazerooni, A. Chu, Biomechanical design of the Berkeley lower extremity exoskeleton (BLEEX). *IEEE/ASME Trans. Mechatron.* **11**, 128–138 (2006). [doi:10.1109/TMECH.2006.871087](https://doi.org/10.1109/TMECH.2006.871087)
70. F. A. Panizzolo, I. Galiana, A. T. Asbeck, C. Siviyy, K. Schmidt, K. G. Holt, C. J. Walsh, A biologically-inspired multi-joint soft exosuit that can reduce the energy cost of loaded walking. *J. Neuroeng. Rehabil.* **13**, 43 (2016). [doi:10.1186/s12984-016-0150-9](https://doi.org/10.1186/s12984-016-0150-9) [Medline](#)
71. Y. Hasegawa, K. Ogura, First report on passive exoskeleton for easy running: PEXER IV. *2013 Int. Symp. Micro-NanoMechatronics Hum. Sci. MHS2013* (2013). [doi:10.1109/MHS.2013.6710481](https://doi.org/10.1109/MHS.2013.6710481).
72. A. J. Young, D. P. Ferris, State of the art and future directions for lower limb robotic exoskeletons. *IEEE Trans. Neural Syst. Rehabil. Eng.* **25**, 171–182 (2017). [doi:10.1109/TNSRE.2016.2521160](https://doi.org/10.1109/TNSRE.2016.2521160) [Medline](#)
73. K. Shamaei, M. Cenciarini, A. A. Adams, K. N. Gregorczyk, J. M. Schiffman, A. M. Dollar, Biomechanical effects of stiffness in parallel with the knee joint during walking. *IEEE Trans. Biomed. Eng.* **62**, 2389–2401 (2015). [doi:10.1109/TBME.2015.2428636](https://doi.org/10.1109/TBME.2015.2428636) [Medline](#)
74. J. M. Donelan, Q. Li, V. Naing, J. A. Hoffer, D. J. Weber, A. D. Kuo, Biomechanical energy harvesting: Generating electricity during walking with minimal user effort. *Science* **319**, 807–810 (2008). [doi:10.1126/science.1149860](https://doi.org/10.1126/science.1149860) [Medline](#)

75. P. Malcolm, W. Derave, S. Galle, D. De Clercq, A simple exoskeleton that assists plantarflexion can reduce the metabolic cost of human walking. *PLOS ONE* **8**, e56137 (2013). [doi:10.1371/journal.pone.0056137](https://doi.org/10.1371/journal.pone.0056137) [Medline](#)
76. J. Zhang, P. Fiers, K. A. Witte, R. W. Jackson, K. L. Poggensee, C. G. Atkeson, S. H. Collins, Human-in-the-loop optimization of exoskeleton assistance during walking. *Science* **356**, 1280–1284 (2017). [doi:10.1126/science.aal5054](https://doi.org/10.1126/science.aal5054) [Medline](#)
77. C. L. Dembia, A. Silder, T. K. Uchida, J. L. Hicks, S. L. Delp, Simulating ideal assistive devices to reduce the metabolic cost of walking with heavy loads. *PLOS ONE* **12**, e0180320 (2017). [doi:10.1371/journal.pone.0180320](https://doi.org/10.1371/journal.pone.0180320) [Medline](#)
78. S. Galle, P. Malcolm, W. Derave, D. De Clercq, Uphill walking with a simple exoskeleton: Plantarflexion assistance leads to proximal adaptations. *Gait Posture* **41**, 246–251 (2015). [doi:10.1016/j.gaitpost.2014.10.015](https://doi.org/10.1016/j.gaitpost.2014.10.015) [Medline](#)
79. R. Margaria, Positive and negative work performances and their efficiencies in human locomotion. *Int. Z. Angew. Physiol.* **25**, 339–351 (1968). [Medline](#)
80. R. W. Jackson, C. L. Dembia, S. L. Delp, S. H. Collins, Muscle-tendon mechanics explain unexpected effects of exoskeleton assistance on metabolic rate during walking. *J. Exp. Biol.* **220**, 2082–2095 (2017). [doi:10.1242/jeb.150011](https://doi.org/10.1242/jeb.150011) [Medline](#)
81. B. R. Umberger, K. G. M. Gerritsen, P. E. Martin, A model of human muscle energy expenditure. *Comput. Methods Biomech. Biomed. Engin.* **6**, 99–111 (2003). [doi:10.1080/1025584031000091678](https://doi.org/10.1080/1025584031000091678) [Medline](#)
82. M. H. Schwartz, A. Rozumalski, J. P. Trost, The effect of walking speed on the gait of typically developing children. *J. Biomech.* **41**, 1639–1650 (2008). [doi:10.1016/j.jbiomech.2008.03.015](https://doi.org/10.1016/j.jbiomech.2008.03.015) [Medline](#)
83. J. R. Koller, D. H. Gates, D. P. Ferris, C. David Remy, Eds., *Robotics: Science and Systems* (Univ. of Michigan, 2016).
84. P. E. di Prampero, G. Atchou, J.-C. Brückner, C. Moia, The energetics of endurance running. *Eur. J. Appl. Physiol. Occup. Physiol.* **55**, 259–266 (1986). [doi:10.1007/BF02343797](https://doi.org/10.1007/BF02343797) [Medline](#)
85. M. Grimmer, R. Riener, C. J. Walsh, A. Seyfarth, Mobility related physical and functional losses due to aging and disease: A motivation for lower limb exoskeletons. *J. Neuroeng. Rehabil.* **16**, 2 (2019). [doi:10.1186/s12984-018-0458-8](https://doi.org/10.1186/s12984-018-0458-8) [Medline](#)
86. D. S. Kim, H.-J. Lee, S.-H. Lee, W. H. Chang, J. Jang, B.-O. Choi, G.-H. Ryu, Y.-H. Kim, A wearable hip-assist robot reduces the cardiopulmonary metabolic energy expenditure during stair ascent in elderly adults: A pilot cross-sectional study. *BMC Geriatr.* **18**, 230 (2018). [doi:10.1186/s12877-018-0921-1](https://doi.org/10.1186/s12877-018-0921-1) [Medline](#)
87. I. Jonkers, S. Delp, C. Patten, Capacity to increase walking speed is limited by impaired hip and ankle power generation in lower functioning persons post-stroke. *Gait Posture* **29**, 129–137 (2009). [doi:10.1016/j.gaitpost.2008.07.010](https://doi.org/10.1016/j.gaitpost.2008.07.010) [Medline](#)
88. F. Porciuncula, R. Nuckols, N. Karavas, C.-K. Chang, T. C. Baker, D. Orzel, D. Perry, T. Ellis, L. Awad, C. Walsh, Assisting limb advancement during walking after stroke using

a wearable soft hip exosuit: A proof-of-concept. *Biosyst. Biorobot.* **21**, 312–316 (2019).  
[doi:10.1007/978-3-030-01845-0\\_63](https://doi.org/10.1007/978-3-030-01845-0_63)